

## Decomposition of 2-chlorophenol by supercritical water oxidation with zirconium corrosion

Jae-Hyuk Lee, Sang-Ha Son, Tran Tan Viet, and Chang-Ha Lee<sup>†</sup>

Department of Chemical and Biomolecular Engineering, Yonsei University, Seoul 120-749, Korea  
(Received 23 June 2008 • accepted 30 September 2008)

**Abstract**—The 2-chlorophenol (2-CP) was oxidized in a continuous anti-corrosive supercritical water system. The variation of decomposition efficiency by the corrosion of zirconium 702 was also studied at the variation of feed concentration and reaction time. According to AES depth profile, the oxygen penetration depth to zirconium was not proportional to the exposure time. It might stem from the formation of zirconium oxide layer on the surface delaying the corrosion. However, the increase in feed concentration accelerated the corrosion of zirconium. The corrosion of zirconium at low feed concentration led to the improvement of decomposition efficiency due to the catalytic effect of formed zirconium oxides, while that at high feed concentration deteriorated the decomposition efficiency owing to large consumption of oxidant in corrosion.

Key words: Supercritical Water Oxidation, Halogenated Compounds, Corrosion, Zirconium

### INTRODUCTION

In recent times attention has been increasingly devoted to supercritical water as a reaction medium. Supercritical conditions may be advantageous for reactions involved in fuels processing, biomass conversion, biocatalysis, homogeneous and heterogeneous catalysis, environmental control, polymerization and materials synthesis [1].

Hazardous organic compounds can be completely oxidized and converted to carbon dioxide (CO<sub>2</sub>) and water (H<sub>2</sub>O) by using an oxidant at above the critical point of water (T<sub>c</sub>=374.3 °C, P<sub>c</sub>=221 bar) [2]. Supercritical water oxidation (SCWO) systems are known as a very efficient way to treat refractory/hazardous compounds, like PCB [3] and Dioxins [4], compared to other feasible technologies, including wet air oxidation. Many researchers have focused on finding variables for the process design by experimenting with various kinds of industrial wastewaters [7,10-15]. However, the applicability of this process hinges not just on its capability to remove the desired level of pollutant, but, more importantly, on its cost effectiveness. Nevertheless, SCWO is an effective technique for the treatment of toxic and refractory compounds.

In general, the desired decomposition and removal efficiency of SCWO can be achieved in a few seconds or minutes [2,4]. However, both corrosion due to acid and fouling due to the low solubility of inorganic salts in the treatment of halogenated compounds need to be taken into account [5,6]. The decomposition of halogenated chlorinated organic compounds in the SCWO process leads to the significant corrosion of equipment, including tubing, due to acidic byproduct [7,8].

To avoid this problem, internal agents or a transpiring wall in the SCWO reactor were introduced [9]. However, it was reported that this can age when exposed to acidic conditions [10]. Neutralizing acids with alkaline solution also leads to the partial or complete

block of the reactor and tubing due to the low solubility of salt in SCWO. Therefore, salt formation in SCWO system remains a fouling issue. Many researchers have focused on solving these problems using a variety of methods and reactor designs [7,10-12]. In addition, various materials have been employed for the construction of SCWO systems [10,13,14]. And the corrosion phenomena of various metal alloys have also been investigated [15] because it is important to select materials suitable for the reactor. However, when the tested materials were oxidized in supercritical conditions, it was difficult to control the corrosion of the reactor itself. It has also been reported that the addition of neutralizers into the SCWO reactor affected the reaction and corrosion [16,17].

Recently, we reported on the continuous anti-corrosive SCWO system, which installed a ceramic tube into a reactor [12]. In addition, zirconium was suggested as one of the candidate metals for the reactor due to its strong corrosion resistance under the SCWO in the previous work [18]. However, the corrosion resistance of zirconium should be tested at various conditions. In addition, the catalytic contribution in SCWO by metal oxide particles, generated by the zirconium corrosion, has to be evaluated for understanding the overall reaction performance.

In this study, the decomposition efficiency of 2-CP by SCWO was measured in the continuous anti-corrosive SCWO system when the zirconium 702 coupon was simultaneously corroded in the system. The effects of feed concentration and reaction time on the decomposition efficiency and corrosion of zirconium were studied.

### EXPERIMENTAL AND ANALYTICAL CONDITIONS

#### 1. Chemicals

The distilled water was purified by using a water deionized purifier; then the treated water was purged by N<sub>2</sub> for 30 min before each experiment. The 2-CP with 99.9% purity (WAKO Pure Chemical Industries, Ltd.) was mixed with primary distilled water as a feed solution of 1,000 ppm and 3,000 ppm. As oxidizing and neutralizing agents, a 100% stoichiometric amount of hydrogen peroxide (H<sub>2</sub>O<sub>2</sub>,

<sup>†</sup>To whom correspondence should be addressed.  
E-mail: leech@yonsei.ac.kr

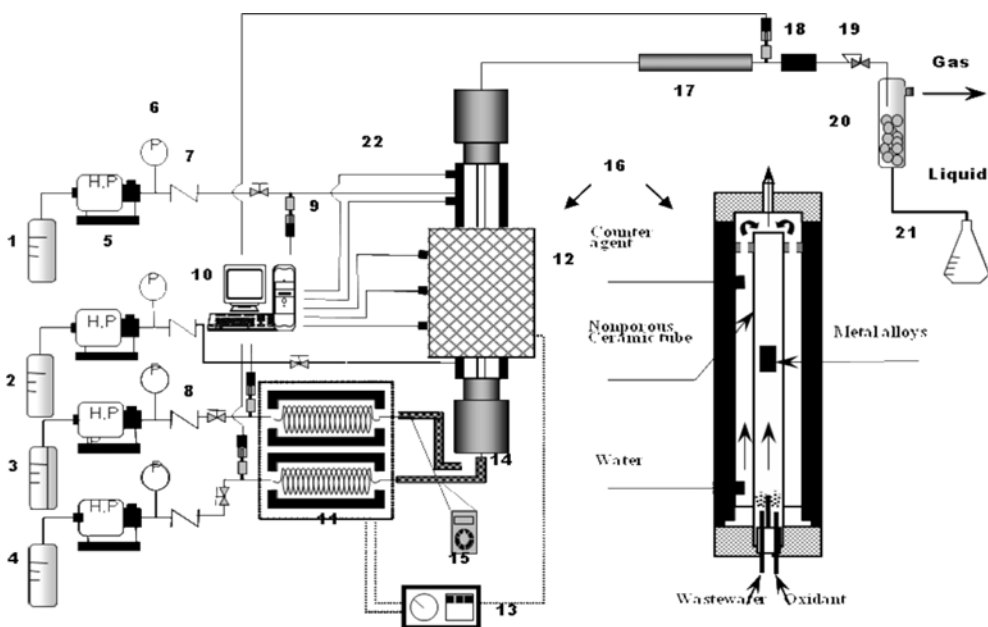
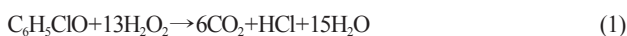


Fig. 1. Schematic of continuous anti-corrosive SCWO reactor system.

- |                         |                        |                              |                             |
|-------------------------|------------------------|------------------------------|-----------------------------|
| 1. Counter agent (NaOH) | 7. Check valve         | 13. Heater controller        | 19. Back pressure regulator |
| 2. Water                | 8. Ball valve          | 14. Heating tape             | 20. Air/water separator     |
| 3. Waste water          | 9. Pressure transducer | 15. Heating tape controller  | 21. Sample tray             |
| 4. Oxidant              | 10. Data saving system | 16. Reactor                  | 22. Thermocouple            |
| 5. High-pressure pump   | 11. Pre-heater         | 17. Condenser (cooling zone) |                             |
| 6. Pressure gauge       | 12. Heater             | 18. Line filter              |                             |

30 wt%, Junsei Chemical. Co., Ltd.) and 200% stoichiometric amount of sodium hydroxide (NaOH, Yakuri Pure Chemicals Co., Ltd.) were used, respectively. The theoretical amount of  $H_2O_2$  and NaOH for the complete neutralization was calculated under the assumption of the complete decomposition of 2-CP in the SCWO as follows:



## 2. Experimental Apparatus and Procedure

The corrosion test was conducted using a continuous anti-corrosive SCWO reactor system, made of stainless steel 316, as shown in Fig. 1. A non-porous ceramic tube (99%  $Al_2O_3$ , 7 mm i.d., 9 mm o.d.) was installed inside the stainless steel reactor in a shell and tube type [12]. Four high pressure pumps (max. 6,000 psi, Lab Alliance, Prep. 100) were used to convey wastewater, oxidant, pure water, and neutralizer, respectively. The flow rates of all influents were set to 2 mL/min.

By using separated lines, the wastewater and oxidant were heated separately to less than 100 °C in a preheating unit and added to the reactor to minimize the corrosion of the inlet lines and the bottom part of the reactor. Since these two influents were mixed inside the ceramic tube after passing the ceramic partition in the reactor, the inlet lines and bottom part of reactor could be protected from corrosion. Simultaneously, at the bottom reactor, pure water was supplied at room temperature to the space between the wall of the vessel and the wall of the nonporous ceramic tube. This was to prevent possible damage of the ceramic tube from pressure difference. In the reactor, the feed was heated to reaction temperature by an electronic heating element (max. 1,300 °C).

The neutralizing NaOH solution was fed into the top of the reac-

tor. The effluent solution from the reactor was mixed with a neutralizer at the part of the reactor cap. Since NaOH solution was supplied at room temperature, it also acted as a cooling agent for the reaction products. Because NaOH can be dissolved at a low temperature solution, fouling problems could be overcome and the neutralizer could contribute to protecting outlet lines from corrosion.

Temperatures were monitored with five thermocouples (K-type) located between the ceramic tube and the metal-shell reactor. Four pressure transducers were located at the inlet lines for the waste water,  $H_2O_2$  and NaOH solutions and at the outlet line after the cooling unit. To maintain the desired pressure in the reactor, a back-pressure regulator (BPR, max. 408 bar, Tescom, USA) with a line filter (0.45  $\mu$ m) was installed in the effluent line. The experimental apparatus and procedure were presented in detail in a previous study [12].

For the corrosion test of alloys under supercritical conditions (380 °C and 250 atm), zirconium 702 was selected as a test alloy. The metal coupons with a total surface area of about 250 mm<sup>2</sup> were located in the middle of the reactor. After reaching the desired temperature and pressure with water, the feed was switched to 2-CP solution and effluent was sampled. The test coupons were kept in a vial filled with nitrogen gas for chemical surface analysis after they were taken out of the reactor.

## 3. Analytical Methods

Decomposition efficiency of each sample was measured by total organic carbon (Total Organic Carbon, SHIMADZU) analysis. Surface chemical analysis of corroded metal alloys was conducted by using AES/SAM (auger electron spectroscopy-scanning auger electron microscopy, Perkin Elmer, PHI model 670). The conditions of the survey scan and sputter depth profile of the AES were recorded

as the following: primary beam energy  $E_p=5$  keV, primary beam current  $I_p=0.01$   $\mu\text{A}$ , and beam diameter  $0.4$   $\mu\text{m}$ . The resolution of the cylindrical mirror analyzer was set to  $0.6\%$ . The argon ion beam, with an ion energy level of  $3$  keV and current density of  $0.6$   $\mu\text{A}/\text{m}^2$ , was produced by a differentially pumped ion gun. The sputter profiles were analyzed with the PC PHI-MATLAB software package. Morphology analysis of the surface of the alloys was done by scanning auger-electron microscopy (SAM).

## RESULTS AND DISCUSSION

### 1. Effect of Reaction Time

All the experiments were performed at  $250$  atm and  $380^\circ\text{C}$ . It was reported that the decomposition of halogenated compound could reach higher than  $99.9\%$  by controlling the operating variables [12, 15]. However, since the effects of experimental variables on de-

composition efficiency were elucidated, the amount of oxidant was controlled to reach the decomposition efficiency of about  $96\%$  in this study.

Figs. 2 and 3 show the AES montage display and the AES depth profiles of zirconium 702 exposed to supercritical water oxidation of 2-CP at different reaction times.

The oxygen peak coexisted with two Zr peaks as shown in Fig. 2. However, the Zr peak on the left side disappeared simultaneously when the oxygen peak disappeared. Then, one Zr peak with high intensity was observed, which implies that the Zr peak on the left side indicates an oxide form of Zr. In addition, a small carbon peak was also monitored in the figure.

In Figs. 3(a) and (b), the oxygen penetration depth was much deeper at the reaction time of 2 hrs than at that of 1 hr. It is noted that the atomic % of oxygen is about  $60$  regardless of the reaction time. The results indicate that the same metal oxides are formed on the sur-

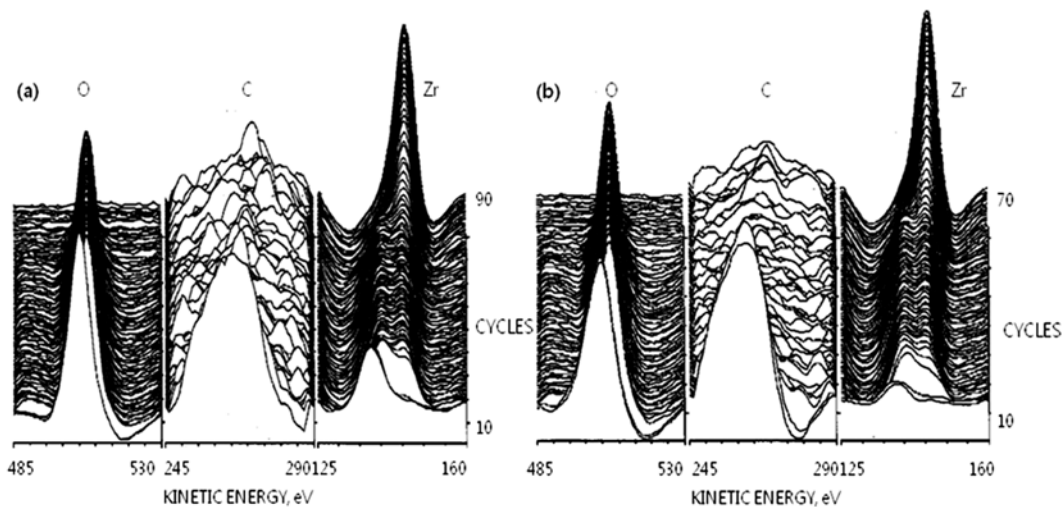


Fig. 2. AES montage display of the surface of zirconium 702 exposed to supercritical water oxidation at different reaction times: (a) 1 hour and (b) 2 hours at  $250$  atm,  $380^\circ\text{C}$ , and 2-CP of  $1,000$  ppm.

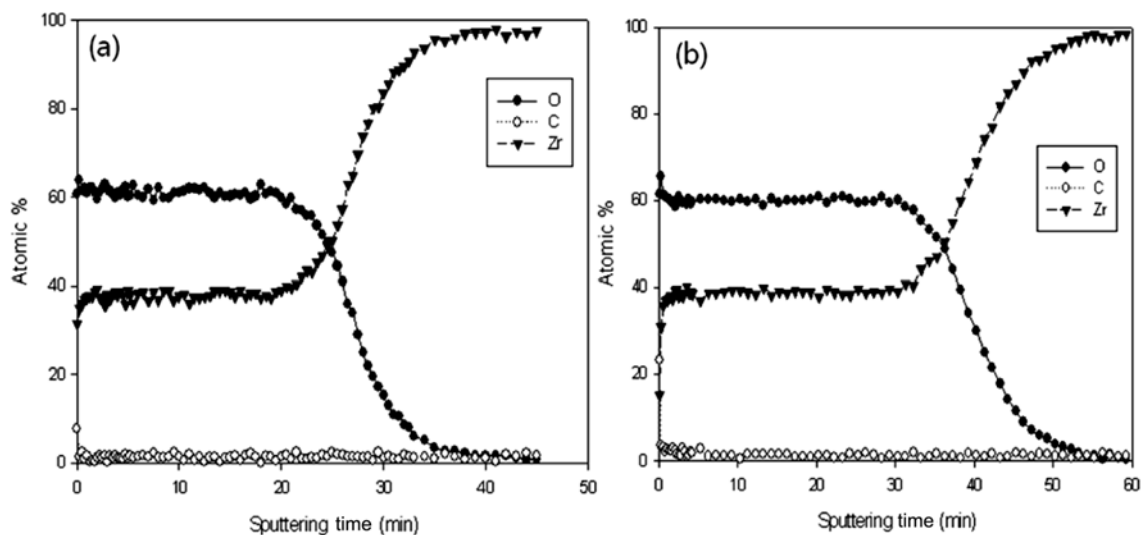


Fig. 3. AES depth profile of zirconium 702 exposed to supercritical water oxidation at different reaction times: (a) 1 hour and (b) 2 hour at  $250$  atm,  $380^\circ\text{C}$ , and 2-CP of  $1,000$  ppm.

face of zirconium, but the only difference between two metal samples is the depth of metal oxide layer.

The sputter rate was a depth of 199 Å/min, based on the SiO<sub>2</sub> in the AES. Therefore, with the sputter rate, the oxygen penetration depth could be calculated [17]. The oxygen penetration depth was 7,761 Å at 1 hr reaction and 10,547 Å at 2 hrs reaction. According to Fig. 3 and calculated results, the corrosion rate of zirconium, exposed for 1 hr at SCWO, was different from that exposed for 2 hrs in the reaction time. It implies that the formed oxide layer might delay the penetration of oxygen to the metal.

Fig. 4 shows the decomposition efficiency of 2-CP for 2 hr reaction time with the corrosion of zirconium coupon at the supercritical condition. Since the feed was mixed to the reactor water at the initial stage, the samples obtained from the reactor were not presented in the figure. As shown in Fig. 4, the decomposition efficiency was slightly decreased with time.

In the previous study [15], it was reported that the metal corro-

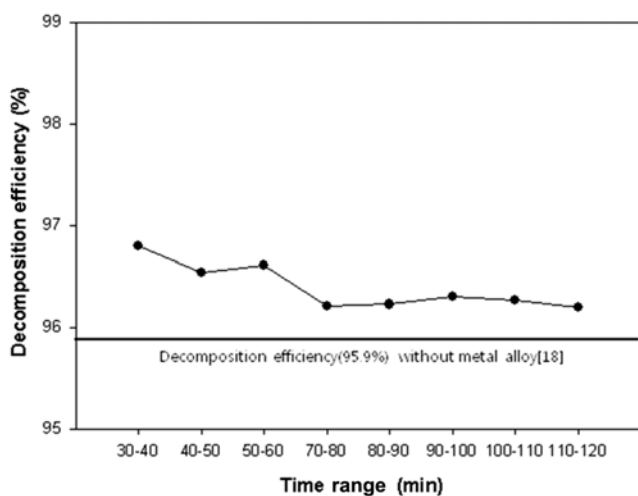


Fig. 4. Decomposition efficiency of 2-chlorophenol with reaction time under corrosion of zirconium at the supercritical condition: 250 atm, 380 °C, and 2-CP of 1,000 ppm.

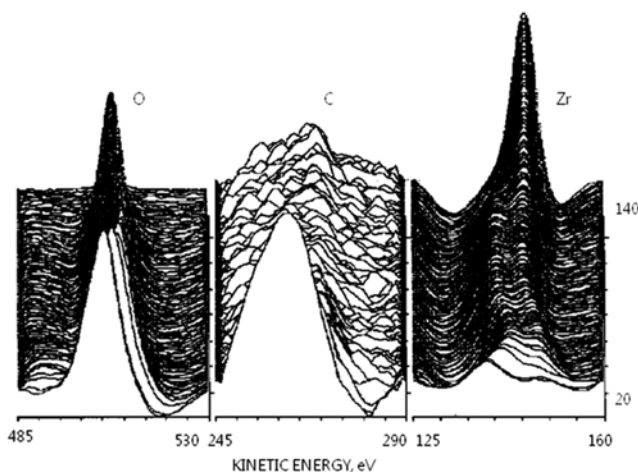


Fig. 5. AES montage display of zirconium 702 exposed to the supercritical condition at 250 atm, 380 °C, 2-CP of 3,000 ppm, and 1 hr reaction time.

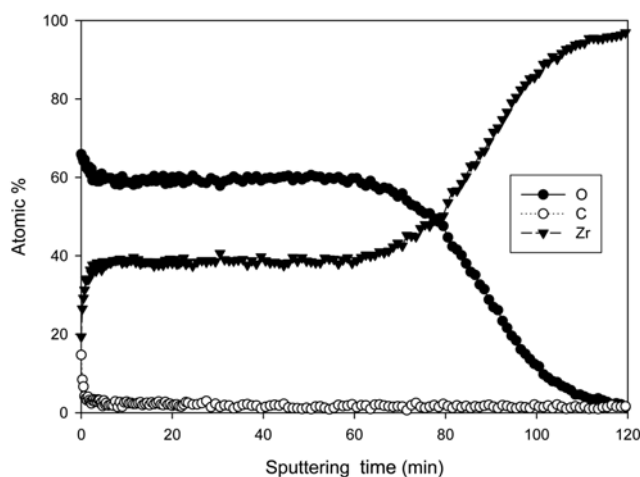


Fig. 6. AES depth profile of zirconium exposed to the supercritical condition at 250 atm, 380 °C, 2-CP of 3,000 ppm, and 1 hr reaction time.

sion led to a decrease of decomposition efficiency because the oxidant was consumed to the corrosion. However, as shown in Fig. 4, the decomposition efficiency with metal corrosion was slightly higher than that without metal corrosion (or without zirconium coupon) in the low feed concentration. It implies that the formed metal oxides contribute to the decomposition of 2-CP at SCWO. Such a phenomenon from relatively low feed concentration could not be observed from the high feed concentration, which is mentioned in a later section.

## 2. Effect of Feed Concentration

Figs. 5 and 6 show the AES depth profile and montage display of zirconium 702 exposed to the SCWO of 2-CP at the high feed concentration (3,000 ppm). The shape of the AES montage display was the same as in the previous results in Fig. 2. However, the oxygen peak and two zirconium peaks disappeared after longer sputtering cycles. Therefore, as can be seen in Fig. 6, the oxygen penetration depth was much deeper at the high feed concentration than at the low feed concentration.

Since the feed concentration increased three times from the low feed concentration, the amount of oxidant (H<sub>2</sub>O<sub>2</sub>) was also increased to three times. Keeping the maximum oxygen atomic% of 60 like the results at the low feed concentration, the oxygen penetration depth (31,044 Å) was almost 4.5 times greater than that at low feed concentration condition. It indicates that more severe condition with respect to feed concentration leads to the acceleration of corrosion of metal.

Fig. 7 shows the decomposition efficiency of 2-CP with corrosion of zirconium at the high feed concentration. The decomposition efficiency at the high feed concentration was in the range of 90-92%. Compared to Fig. 4, the decomposition efficiency was significantly decreased to the lower level than the reaction without metal alloy. In addition, the decrease of decomposition efficiency with time was similar to the case of low feed concentration. The severe corrosion of metal resulted in a large amount of oxidant consumption. Because the concentration of oxidant had significant effects on the decomposition efficiency in the continuous SCWO system [12], the contribution of the formed metal oxides to the reaction

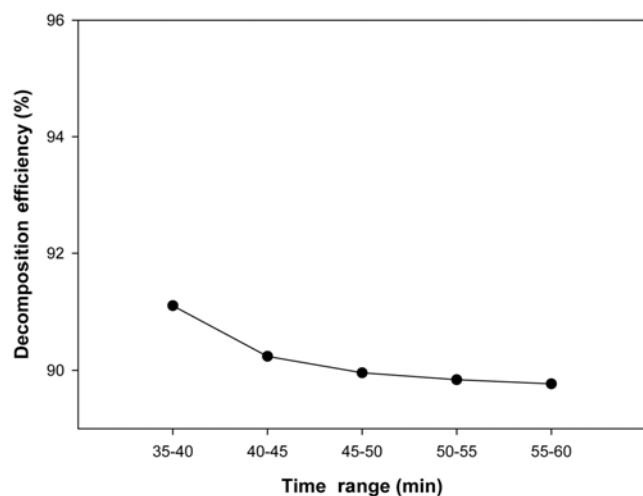


Fig. 7. Decomposition efficiency of 2-chlorophenol with corrosion of zirconium at the supercritical condition: 250 atm, 380 °C, 2-CP of 3,000 ppm, and 1 hr reaction time.

became negligible, unlike the result in the low feed concentration.

### CONCLUSION

The 2-CP was decomposed under the corrosion of zirconium 702 in a continuous anti-corrosive SCWO system. Through the surface chemical analysis of the corroded zirconium exposed to the SCWO, it was found that the oxygen penetration depth was much deeper at the reaction time of 2 hrs than at that of 1 hr. However, the atomic% of oxygen was about 60 regardless of the reaction time and the same metal oxides were formed on the surface of zirconium. The corrosion rates of zirconium between 1 hr and 2 hrs at SCWO reaction time were different from each other. On the other hand, more severe condition with respect to feed concentration led to the acceleration of corrosion of metals.

To sum up, the corrosion of zirconium at low feed concentration led to the improvement of decomposition efficiency due to the catalytic work of formed zirconium oxides. However, high feed concentration deteriorated the decomposition efficiency owing to large consumption of oxidant in corrosion. In addition, the decomposition efficiency was slightly decreased with time, which was independent of feed conditions.

### ACKNOWLEDGMENTS

The authors gratefully acknowledge the financial support from the Ministry of Environment for the Eco-technopia 21 Project.

### REFERENCES

1. P. E. Savage, S. Gopalan, T. I. Mizan, C. J. Martino and E. E. Brock, *AIChE J.*, **41**, 1723 (1995).
2. K. Peter and D. Eckhard, *Chem. Eng. J.*, **83**, 207 (2001).
3. K. Hatakeda, Y. Ikushima, O. Sato, T. Aizawa and N. Saito, *Chem. Eng. Sci.*, **54**, 3079 (1999).
4. T. Sako, T. Sugeta, K. Otake, M. Sato, M. Tsugumi, T. Hiaki and M. Hongo, *J. Chem. Eng. Jpn.*, **30**, 744 (1997).
5. P. Kritzer, N. Boukis and E. Dinjus, *Corrosion*, **54**, 824 (1998).
6. L. B. Kriksunov and D. Macdonald, *J. Electrochem. Soc.*, **142**, 4069 (1995).
7. V. Casal and H. Schmidt, *J. Supercrit. Fluids*, **13**, 269 (1998).
8. K. P. Johnston and J. B. Chlistunoff, *J. Supercrit. Fluids*, **12**, 155 (1998).
9. J. C. Meyer, P. A. Marrone and J. W. Tester, *AIChE J.*, **41**, 2108 (1995).
10. P. Muthukumaran and B. Ram. Gupta, *Ind. Eng. Chem. Res.*, **39**, 4555 (2000).
11. P. J. Crooker, K. S. Ahluwalia, Z. Fan and J. Prince, *Ind. Eng. Chem. Res.*, **39**, 4865 (2000).
12. H. C. Lee, J. H. In, J. H. Kim and C. H. Lee, *J. Supercrit. Fluids*, **36**, 59 (2005).
13. B. R. Foy, K. Waldthausen, M. A. Sedillo and S. J. Buelow, *Environ. Sci. Technol.*, **30**, 2790 (1996).
14. N. Boukis, N. Claussen, K. Ebert, R. Janssen and M. Schacht, *J. Eur. Ceram. Soc.*, **17**, 71 (1999).
15. H. C. Lee, S. H. Son, K. Y. Hwang and C. H. Lee, *Ind. Eng. Chem. Res.*, **45**, 3412 (2006).
16. G. Lee, T. Nunoura, Y. Matsumura and K. Yamamoto, *J. Supercrit. Fluids*, **24**, 239 (2002).
17. S. H. Son, J. H. Kim, H. C. Lee and C. H. Lee, *Korean J. Chem. Eng.*, **23**, 385 (2006).
18. S. H. Son, J. H. Lee and C. H. Lee, *J. Supercrit. Fluids*, **44**, 370 (2008).